Journal of The Electrochemical Society, **147** (11) 4268-4272 (2000)
S0013-4651(99)12-019-6 CCC: $7.00

Reliability of Fluorinated Silicon Oxide Film Prepared by Temperature Difference-Based Liquid Phase Deposition

Ching-Fa Yeh,[z] Yueh-Chuan Lee,* and Su-Chen Lee

Department of Electronics Engineering and Institute of Electronics, National Chiao Tung University, Hsinchu, Taiwan

Fluorinated silicon oxide film prepared by using temperature difference-based liquid phase deposition is very potential for use as an intermetal dielectric owing to its high fluorine concentration (8.6 atom %), low dielectric constant (3.46), low stress (41 MPa), low leakage current density (4.6×10^{-9} A/cm^2 at 2 MV/cm), and low deposition temperature (room temperature). In this work, we closely examine reliability issues including resistance to water absorption and thermal stability by adopting the repeatedly annealing (400°C) and boiling test. After the test, the net increase in the dielectric constant is only 0.02; the stress changes within −24 to 41 MPa with a resultant zero stress; the leakage current density increases slightly to 8.0×10^{-9} A/cm^2. Obviously the film will preserve its attractive properties in a back-end process similar to the test. Accompanied with the investigation of p-etch rate, thermal desorption spectroscopy, and Fourier transform infrared spectroscopy, a feasible mechanism that accounts for the variation of the properties during the test is proposed. A high temperature (>400°C) annealing effect is also studied. The film is thermally stable up to 600°C, which is limited by the decomposition of Si–F bonds. The thermal stability of 600°C is obviously sufficient for intermetal dielectric application.

Manuscript received December 6, 1999.

As device geometry is scaled down to deep submicrometer region, the parasitic capacitance between closely spaced metal lines becomes important in the issue of resistance-capacitance time delay.[1] Meanwhile, high stress in the intermetal dielectric (IMD) film also degrades the reliability of interconnects.[2,3] Especially the problem becomes more serious if the deposition temperature of IMD is high.[3] Therefore, for scaling down devices, a novel IMD with low dielectric constant, low stress, and low deposition temperature is essential. The fluorinated oxide film prepared by conventional liquid phase deposition (C-LPD) with adding boric acid or water as a supersaturation initiator was verified to meet the requirements.[4-8]

For the C-LPD film, the fluorine concentration has been shown to increase with the decreasing quantity of supersaturation initiator.[9] Therefore, the quantity of supersaturation initiator should be reduced for increasing the fluorine concentration and reducing the dielectric constant. However, the deposition rate, which decreases as the quantity of initiator decreases, become a limiting factor while increasing the fluorine concentration.[10] The fluorine concentration of C-LPD film at most achieves 6.25 atom %.[9]

Sakai *et al*. first proposed the notion of controlling the degree of supersaturation for the deposition solution by changing the deposition temperature from the solution-preparation temperature, instead of adding any supersaturation initiator.[11] Kawahara *et al*. studied the chemical composition, the p-etch rate and the stress for this kind of oxide films prepared by using 2-3 M H_2SiF_6.[12] According to their results, a higher H_2SiF_6 concentration, *i.e.*, 3 M, led to a higher film density and a higher fluorine concentration. In this work, using a nondiluted (4 M) H_2SiF_6 solution and the temperature difference technique proposed by Sakai *et al*., the LPD method is expected promising in preparing highly fluorinated film. This method is termed temperature difference-based LPD (TD-LPD).

Oxide films with high fluorine concentrations are generally hygroscopic, *i.e.*, the film properties easily change after moisture stress and/or thermal annealing.[5,6] To apply the TD-LPD film as an IMD, the reliability issues must be clarified in advance. Since an IMD may be thermally treated and exposed to moist ambient more than once, the reliability of the film is thus studied through evaluating physicochemical and electrical properties during the test of repeated annealing (400°C) and boiling (in 100°C water). A feasible mechanism that accounts for the variation of the properties during the test is proposed. High temperature (>400°C) stability of the film is also evaluated.

* Electrochemical Society Student Member.
[z] E-mail: cfyeh@cc.nctu.edu.tw

Experimental

Preparation of TD-LPD film.—Silica powder was added to a 4 M H_2SiF_6 solution and then dissolved by stirring at ~0°C for 24 h. After removing the undissolved silica by filtering, the saturated solution was heated to 25°C, and became supersaturated. After cleaning, the wafers were immersed in the solution and, then, the TD-LPD film was gradually deposited on the wafers. Thus, the difference between the solution preparation temperature and the deposition temperatures was 25°C.

Reliability test.—Reliability of the TD-LPD film was evaluated by using (*i*) repeatedly annealing and boiling test (RABT), and (*ii*) high temperature (400-800°C) annealing in N_2 for 30 min. Figure 1 is the RABT flow diagram with denotation of films at different stages. The film before any treatment is denoted as the as-deposited film. The as-deposited film processed with the first annealing at

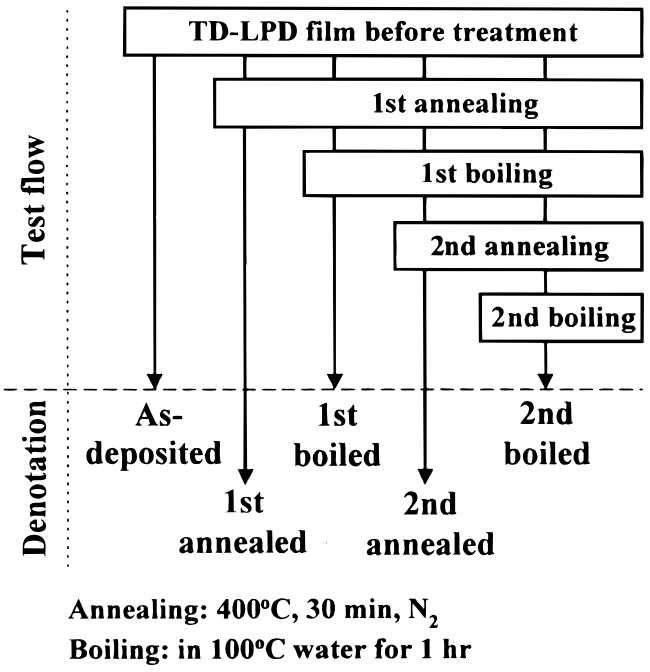

Figure 1. RABT flow diagram with denotation of films at different stages.

S0013-4651(99)12-019-6 CCC: $7.00

Table I. Properties of films prepared at room temperature by TD-LPD, C-LPD, ECR-CVD, and RT-CVD.

	TD-LPD	C-LPD	ECR-CVD	RT-CVD
F concentration	8.6 atom %	1.86-6.25 atom %	8.55%[a]	5.3×10^{21} atom/cm^3
Dielectric constant	3.46	3.52∼4.23	3.17	3.7
Stress (MPa)	41	83∼107	−74.2	50
Current density at 2 MV/cm (A/cm^2)	4.6×10^{-9}	2×10^{-9} to 6×10^{-8}	$\sim 2 \times 10^{-6}$	$\sim 4 \times 10^{-7}$

[a] Ratio of FTIR peak intensity (Si–F/Si–O).

400°C for 30 min in N_2 is denoted as the first annealed film; while the as-deposited film processed with first annealing and first boiling stress in 100°C water for 1 h is denoted as the first boiled film. The second annealed and the second boiled films also denote the films after second annealing and second boiling, respectively.

Measurements.—The dielectric constant (1 MHz) was determined by C-V measurement through the metal oxide semiconductor (MOS) capacitor structure (A1/110) nm oxide/p-Si). The stress of ∼260 nm thick film was calculated from measured curvature based on Stoney's equation using a Tencor FLX-2320 instrument. The characteristic of current density *vs*. electrical field (J-E) was measured using HP4145B system also with the MOS capacitor, where the Al electrode was negatively biased. Etch rate of the film using p-etch solution ($HF:HNO_3:H_2O = 3:2:60$) was employed to investigate the film density. The desorbed species, including H_2O and HF during heating, were monitored by using thermal desorption spectroscopy (TDS). The content of the Si–F bond was evaluated by Fourier transform infrared spectroscopy (FTIR).

Results and Discussion

As listed in Table I, fluorine concentration, dielectric constant, stress, and leakage current density (2 MV/cm) of as-deposited TD-LPD film are 8.6 atom %, 3.46, 41 MPa, and 4.6×10^{-9} A/cm^2, respectively. Properties of films prepared at room temperature by C-LPD,[7-9,13] electron cyclotron resonance chemical vapor deposition (ECR-CVD)[14,15] and room temperature chemical vapor deposition (RT-CVD)[5,16] are also listed in Table I for comparison, where C-LPD films are prepared by using water as the supersaturation initiator. Compared with C-LPD film, TD-LPD film exhibits higher fluorine concentration, lower dielectric constant, lower stress, and comparable leakage current level. Compared with ECR-CVD and RT-CVD films, TD-LPD film demonstrates much better insulating property in terms of two orders of magnitude lower leakage current density. TD-LPD film seems very potential for IMD application in terms of its attractive properties.

Figure 2 shows the dielectric constant of the film during RABT. The dielectric constant changes in the range of 3.33-3.48. After the test, the dielectric constant increases only by 0.02. This result reveals that the film can well preserve the merit of low dielectric constant in a back-end process similar to the test.

During the first annealing and boiling cycle, the dielectric constant first decreases from 3.46 to 3.33, then it increases back to 3.46, implying that some polar H_2O species in the film are first removed and then refilled. In fact, H_2O species in a fluorinated oxide film have been recognized as absorbed molecular H_2O in the pore structure, hydrogen-bonded H_2O to Si–OH, and H_2O associated Si–OH bonds, where the former two H_2O species can be removed by 400°C annealing.[17,18] Therefore, desorption/absorption of the two H_2O species accounts for the variation in the dielectric constant in the first cycle. In addition, the Si–OH bond density after the first boiling is not expected to be increased, because the dielectric constant of the first boiled film is not higher than that of the as-deposited film. However, the dielectric constant of the second annealed film becomes higher than that of the first annealed film. This result implies that additional Si–OH bonds, which are thermally stable beyond 400°C, are generated during the second annealing.

In addition to the annealing effect, the first annealed and the second annealed films also differ with respect to variation in the dielectric constant after the subsequent boiling. The increase in the dielectric constant after the second boiling (Δk_2) is smaller than that after the first boiling (Δk_1). This fact indicates that resistance to H_2O absorption for the second annealed film is better than that for the first annealed film. Obviously, the dielectric constant tends to vary less in the latter annealing and boiling cycle. However, the mechanism that the second annealed film has an improved resistance to H_2O absorption is still not clear.

The stress, which is also referred to as the total stress, is also studied. According to Fig. 3, during the test, the total stress varies within −24 to 41 MPa; after the test is becomes nearly zero, *i.e.*, free of stress. This finding reveals that for TD-LPD film, the low stress merit can obviously be preserved after annealing and boiling cycles. In fact, the total stress is the sum of thermal stress and intrinsic stress. For the as-deposited film, the thermal stress is zero since the film is deposited at room temperature. After first annealing, the change in stress is −63 MPa, which is close to the calculated thermal stress (−78 MPa at 400°C).[8] Therefore, the variation in the stress after the first annealing is mainly attributed to the thermal stress induced during the annealing process. The stress remains almost unchanged after (the first or second) boiling. Notably, the stress increases by about 32 MPa after the second annealing. Since Si–OH bonds may be generated during the second annealing, the increased (tensile) stress is presumably due to the formation of additional Si–O–Si bonds between Si–OH bonds. Meanwhile, the film must also be densified with the increasing S–O–Si bond density. These references are examined using a p-etch rate test and TDS.

The p-etch rate for the second annealed film is 12.3 Å/s, which is lower than 13.5 Å/s for the first annealed film by 8.9%, indicating that the second annealed film is more densified. Because the second annealed film is annealed in 400°C ambient for totally 1 h (first annealing + second annealing), one may suspect that longer anneal-

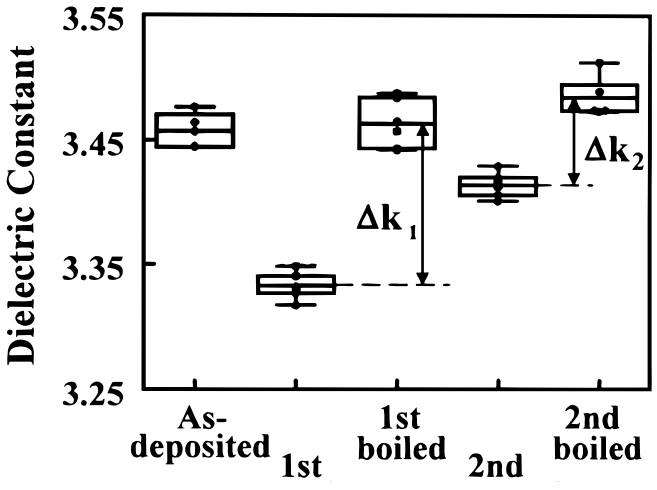

Figure 2. Dielectric constant of TD-LPD film during RABT.

S0013-4651(99)12-019-6 CCC: $7.00

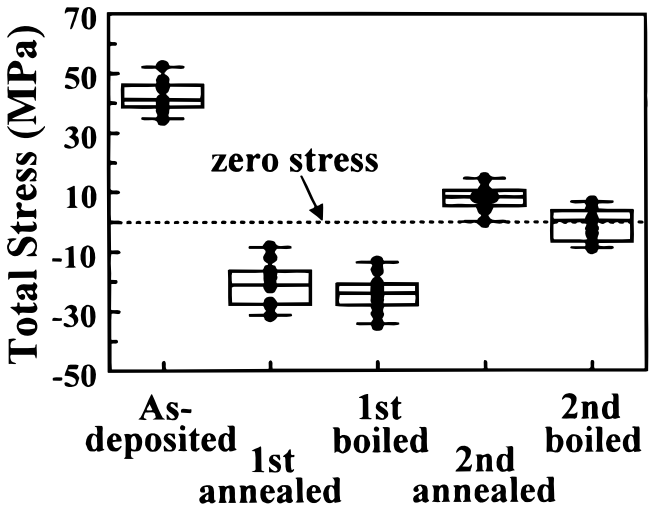

Figure 3. Total stress of TD-LPD film during RABT.

ing time makes the film more dense. The p-etch rate for the first annealed film with further 30 min annealing (without and boiling) is thus investigated and found to be 13.6 Å/s, which is close to that for the first annealed film. This further annealing cannot make the first annealed film more dense. Therefore, the H_2O molecules absorbed by the film during the first boiling must play an important role in enhancing the generation of the additional Si–OH bonds, and the subsequent densification of film.

Figure 4a shows the J-E curves for, in an increasing order of current density, as-deposited, second annealed, second boiled, first boiled, and first annealed films. The breakdown fields for various films are within 6.4-7.7 MV/cm, much higher than the operation field applied to an IMD. Figure 4b shows the distributions of current density at 2 MV/cm for various films. The medium current density (J_{50}) for the as-deposited film is 4.6×10^{-9} A/cm^2. After the first annealing, the J_{50} increases by a factor of 5 to 2.3×10^{-8} A/cm^2. The increase in J_{50} may be attributed to decomposition of weak S–F bonds and/or Si–OH bonds during first annealing with the generation of dangling bonds, which are electrically active traps.[15,19] After the first boiling, the J_{50} decreases to 1.2×10^{-8} A/cm^2, implying that a part of dangling bonds is passivated by water or related species.[19-21] After the second annealing, the J_{50} further decreases to 7.0×10^{-9} A/cm^2. This decrease in J_{50} is attributable to that the film becomes densified. The densified film is very stable in electrical insulating property in terms of scant variation in J_{50} after further (second) boiling.

So far, we have inferred that the film becomes densified after the second annealing, in terms of increased stress, reduced p-etch rate and stabilized insulating property. However, the densification process has not been well understood. Therefore, we use TDS to investigate the process. As mentioned previously, there are three H_2O species in a fluorinated oxide film. HF may also desorb accompanying the desorption of H_2O.[18] We thus monitored desorbed species of H_2O and HF. A heating recipe for TDS measurements is designed so that the heating temperature increases from ~40 to 400°C at a speed of 40°C/min, and maintains at 400°C for 30 min, then increases to ~800°C at the same rate. The holding of temperature at 400°C for 30 min is to simulate the first or the second annealing of RABT. The heating at >400°C is to monitor Si–OH bonds.

Figure 5 shows the TDS spectra for the as-deposited film. Obviously, there are three H_2O (m/e = 18) peaks and three HF (m/e = 20) peaks in the spectra. Each of the three HF peaks appears to correspond to one H_2O peak. In addition, we also find that (*i*) the intensity of every HF peak is weaker than that of the corresponding H_2O peak, and (*ii*) the evolution of every HF peak lags behind that of the corresponding H_2O peak. We therefore inferred that the H_2O molecules react with Si–F bonds in the film during heating, and drives HF desorption together with generation of Si–OH bonds. In fact, the first HF peak (at ~248°C), which is driven by the most intense water desorption (H_2O in the pore structure), is the most faint, revealing that a higher temperature is required to generate Si–OH bonds. This finding accounts for that the Si–OH bond density in the film is not increased by 100°C boiling treatment. When the film is annealed below 400°C, the generation of Si–OH bonds is mainly driven by hydrogen-bonded H_2O. The hydrogen bond between H_2O and Si–OH breaks early from ~290°C, as expressed in Eq. 1

$$\underset{\text{Hydrogen bond}}{\text{Si–OH}\cdots\cdots\cdots\text{H}_2\text{O}} \rightarrow \underset{\text{Broken}}{\text{Si–OH}\cdot\cdot/\!/\cdot\cdot\text{H}_2\text{O}\uparrow} \qquad [1]$$

The desorbed H_2O molecules in Reaction 1 can react later with Si–F bonds, leading to formation of Si–OH bonds and desorption of HF from ~320°C. This is hydrolysis of Si–F bonds, as expressed in Eq. 2

$$\text{Si–F} + \text{H}_2\text{O} \rightarrow \text{Si–OH} + \text{HF}\uparrow \qquad [2]$$

The TDS measurement for the first boiled film can be used to investigate the species desorbed from the film during the second annealing, as shown in Fig. 6. The TDS spectra beyond 400°C are not shown. The spectra closely resemble those of the as-deposited film except that (*i*) earlier evolution of the first and the second H_2O

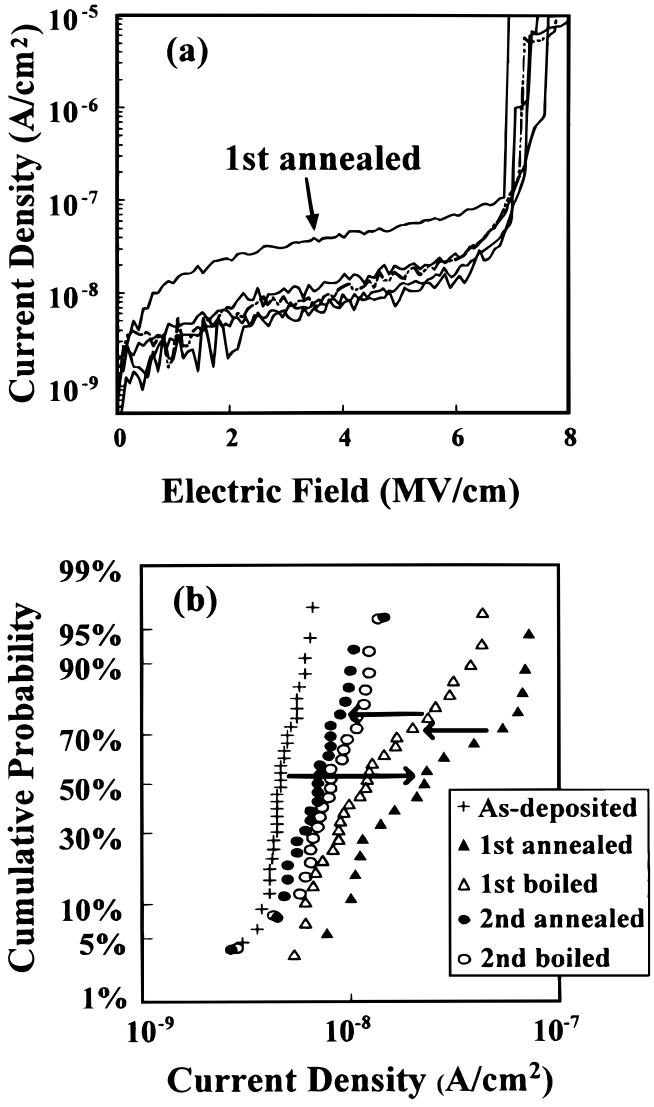

Figure 4. (a) The curves of current density *vs.* electrical field, and (b) the distributions of current density at 2 MV/cm, for various films.

S0013-4651(99)12-019-6 CCC: $7.00

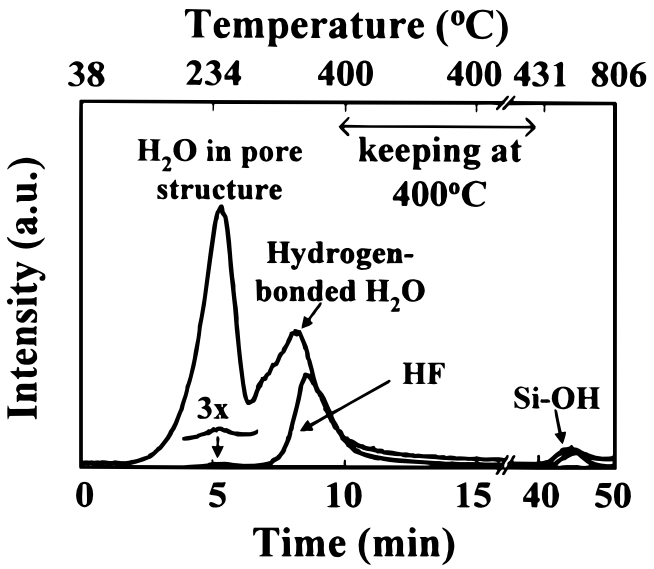

Figure 5. TDS spectra for the as-deposited film with a thickness of 260 nm. The first HF peak has been magnified by 3 times (3x) and replotted in the inset.

peaks, and (*ii*) the shoulder peaks at ~370°C. The earlier evolution may be attributed to that the distribution of water in the first boiled film is closer to the surface than that in the as-deposited film. Since less time is required for the H_2O molecules from the first boiled film to diffuse out to be detected, the evolution of the two H_2O peaks seems earlier. On the other hand, the shoulder peaks are induced by the evolution of another water source with desorption of corresponding HF. In fact, generation of the shoulder peaks is a result of film densification, as explained below.

During the second annealing, Si–OH bonds generated via Reaction 2 keep accumulating from ~300°C since the hydrolysis reaction occurs again. However, as the Si–OH bond density becomes sufficiently high, the neighboring Si–OH bonds can begin to react, resulting in formation of additional Si–O–Si bonds and additional desorption of H_2O. Such a formation accounts for why additional water is desorbed at ~370°C. Notably, the additional formation of Si–O–Si bonds can induce additional tensile stress and densifies the film.[8] Thus, after the second annealing, the increased tensile stress is a result of the dehydration reaction as stated in Eq. 3

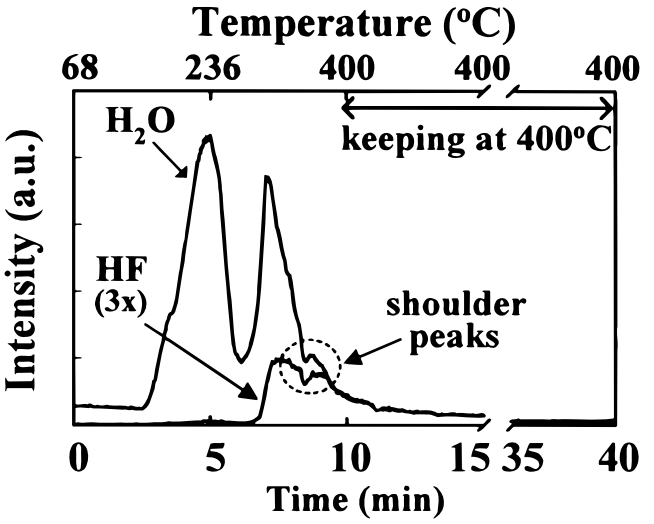

Figure 6. TDS spectra for the first boiled film with a thickness of 260 nm. The HF spectrum has been magnified by 3 times (3x).

$$\text{Si–OH} + \text{Si–OH} \rightarrow \text{Si–O–Si} + H_2O\uparrow + \text{tensile stress} \quad [3]$$

The desorbed water in Eq. 3 again drives HF evolution, forming the HF shoulder peak. The detailed reactions that make the film densified have been well clarified by Eq. 1-3.

Generally, FSO film properties are closely correlated with the fluorine content in the film.[9,15,22] To monitor the relative variation in the amount of Si–F bond during RABT, we calculate the Si–F peak area ratio as an index by dividing the area under Si–F peak (at ~930 cm^{-1}) of FTIR spectrum for treated film to that for the as-deposited film. Figure 7 shows the Si–F peak area ratio during RABT. After the first annealing, the ratio decreases to ~93.5%, revealing that weak Si–F bonds have been removed. The ratio decreases very slightly to ~91.8% after all the subsequent treatments, indicating that most S–F bonds are preserved in the treated film. Therefore, during the test, the TD-LPD film can preserve merits of low dielectric constant, low stress, and low leakage current.

High Temperature Stability

The Si–F peak area ratio for the film after high temperature (400-800°C) annealing was also calculated to evaluate the high temperature stability. As shown in Fig. 8, the Si–F peak area ratio decreases slightly from 93.5 to 87.9%, as the temperature increases from 400 to 600°C; it decreases rapidly to 68.7 and 28.5% as the temperature increases to 700 and 800°C, respectively. This figure indicates that the films are thermally stable up to 600°C, which is limited by the decomposition of Si–F bonds. Since the back-end process temperature is within 400-450°C, the thermal stability of 600°C for TD-LPD film can be concluded excellent for IMD application.

Conclusion

Properties of TD-LPD FSG film during RABT have been investigated. During the test, the dielectric constant changed within 3.33-3.48; the stress varies within −24 to 41 MPa with a resultant zero stress after the test; the leakage current density at 2 mV/cm varies within 4.6×10^{-9} to 2.3×10^{-8} A/cm^2. Obviously, the film can well preserve the merits of low dielectric constant, low stress, and low leakage current level in a back-end process similar to the test. On the other hand, FTIR data show that the film is thermally stable up to 600°C, which is limited by the decomposition of Si–F bonds. The thermal stability of 600°C is obviously sufficient for IMD appli-

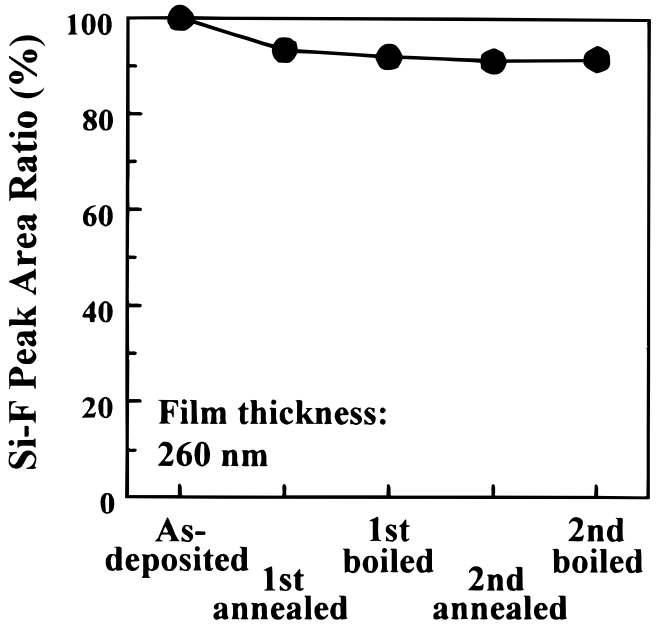

Figure 7. Si–F peak area ratio during RABT.

S0013-4651(99)12-019-6 CCC: $7.00

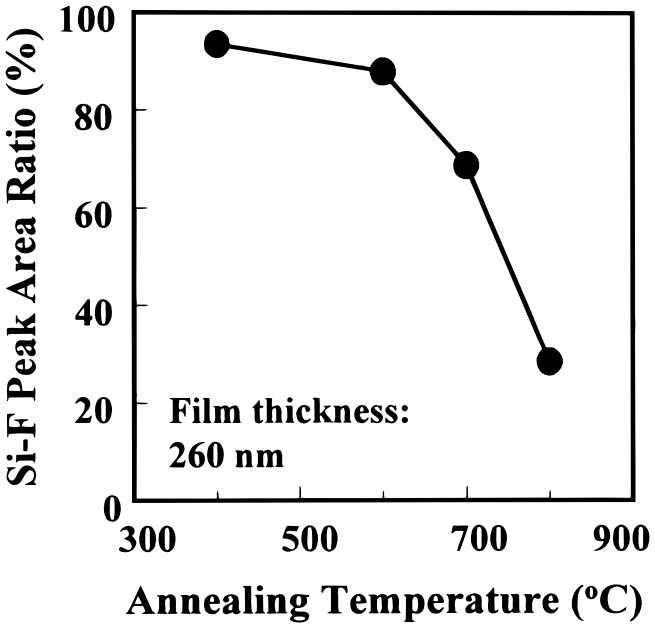

Figure 8. Si–F peak area ratio as a function of annealing temperature.

cation. We thus conclude that the film is very promising as an IMD in terms of its stability.

The variations in the dielectric constant, stress, and leakage current during RABT have also been clarified. During the second annealing, the hydrolysis reaction driven by the desorbed hydrogen-bonded H_2O generates additional Si–OH bonds from ~300°C, leading to a slight increase in the dielectric constant; the dehydration reaction, which occurs from ~370°C between Si–OH bonds, then induces tensile stress and film densification. The densification process also reduces the leakage current density. Besides, the densified film does not easily absorb water during subsequent boiling, resulting in the improved resistance to H_2O absorption and the stabilized dielectric constant.

Acknowledgments

The authors would like to thank the National Science Council, Republic of China, for financially supporting this research under contract no. NSC 89-2215-E-009-006. Stephen Cheng, Joey Chang, and Daniele Change of QRA/Mosel Vitelic Inc. are appreciated for their assistance in analyzing films by TDS.

National Chiao Tung University assisted in meeting the publication costs of this article.

References

1. M. T. Bohr, in *Tech. Dig. Int. Electron Devices Meet*., 241 (1995).
2. J. T. Yue, W. P. Funsten, and R. V. Taylor, *Proceedings of the 23th Annual IEEE International Reliability Physics Symposium*., p. 126 (1985).
3. L. A. Miller and A. K. Stamper, No. 95-ISMIC-10419510369, in *Proceedings of the 12th International VLSI Multilevel Interconnection Conference*, (VMIC), p. 369, June 27-29 (1995).
4. T. Homma and Y. Murao, *Thin solid Films*, **249**, 15 (1994).
5. T. Homma, *J. Non-Cryst. Solids*, **187**, 49 (1995).
6. T. Homma, *Thin Solid Films*, **278**, 28 (1996).
7. S. S. Lin, Ph.D. Thesis, Institute of Electronics, National Chiao Tung University, Hsinchu, Taiwan (1996).
8. C. F. Yeh, S. S. Ling, and W. Lur, *J. Electrochem. Soc*., **143**, 2658 (1996).
9. C. F. Yeh and C. L. Chen, *J. Electrochem. Soc*., **142**, 3579 (1995).
10. C. F. Yeh, C. L. Chen, and G. H. Lin, *J. Electrochem. Soc*., **141**, 3177 (1994).
11. Y. Sakai, T. Goda, A. Hishinuma, and H. Kawahara, *Proceedings of the International Ceramics Conference*, AUSTCE AM 90, Australian Ceramic Society, p. 474, Aug 26-31 (1990).
12. H. Kawahara, Y. Sakai, T. Goda, A. Hishinuma, and K. Takamura, in *Glasses for Optoelectronics II*, Vol. 1513, SPIE, p. 198 (1991).
13. T. Y. Hong, M.S. Thesis, Institute of Electronics, National Chiao Tung University, Hsinchu, Taiwan (1994).
14. K. M. Chang, S. W. Wang, C. J. Wu, T. H. Yeh, C. H. Li, and J. Y. Yang, *Appl. Phys. Lett*., **69**, 1238 (1996).
15. K. M. Chang, S. W. Wang, T. H. Yeh, C. H. Li, and J. J. Luo, *J. Electrochem. Soc*., **144**, 1754 (1997).
16. T. Homma, R. Yamaguchi, and Y. Murao, *J. Electrochem. Soc*., **140**, 687 (1993).
17. M. Yoshimaru, S. Koizumi, K. Shimokawa, and J. Ida, in *Proceedings of the 35th Annual IEEE International Reliability Physics Symposium*, p. 234 (1997).
18. P. W. Lee, S. Mizuno, A. Verma, and H. Tran, and B. Nguyen, *J. Electrochem. Soc*., **143**, 2015 (1996).
19. A. Yokozawa and Y. Miyamoto, *Appl. Phys. Lett*., **73**, 1122 (1998).
20. J. Takahashi, K. Machida, N. Shimoyama, and K. Minegishi, No. 92-ISMIC-10119210331, in *Proceedings of the 9th International VLSI Multilevel Interconnection Conference*, (VMIC), p. 331, June 9-10 (1992).
21. J. Takahashi, K. Machida, N. Shimoyama, and K. Minegishi, *Appl. Phys. Lett*., **62**, 2365 (1993).
22. S. W. Lim, Y. Shimogaki, Y. Nakano, K. Tada, and H. Komiyama, *J. Electrochem. Soc*., **144**, 2531 (1997).